



Construction of heterogeneous Ni catalysts from supports and colloidal nanoparticles – A challenging puzzle

Roberto Rinaldi^{a,*}, Andréia de Melo Porcari^a, Tulio C.R. Rocha^a, Wellington Henrique Cassinelli^b, Renata Uema Ribeiro^b, José Maria Correa Bueno^b, Daniela Zanchet^{a,**}

^a Brazilian Synchrotron Light Laboratory – LNLS, P.O. Box 6192, 13087-500 Campinas, SP, Brazil

^b Department of Chemical Engineering, Federal University of São Carlos, P.O. Box 676, 13565-905 São Carlos, SP, Brazil

ARTICLE INFO

Article history:

Received 5 October 2008
Received in revised form 26 October 2008
Accepted 2 November 2008
Available online 11 November 2008

Keywords:

Ni catalysts
Ni nanoparticles
Colloidal synthesis
Impregnation

ABSTRACT

Well-defined nanoparticles obtained by modern wet chemical synthesis methods can be very useful building blocks for construction of model heterogeneous catalysts. Here we show the challenges involved in the construction of heterogeneous Ni catalysts from supports and colloidal nanoparticles. Surprisingly, “1 + 1” is not equal to “the best catalyst”, following this concept. The thought-provoking lack of catalytic activity of supported Ni NPs in the hydrogenation of cyclohexene and the low activity of these materials in the steam reforming of ethanol were analyzed in details by TEM, XPS, DRIFTS and CO adsorption experiments. The factors responsible for the low catalytic activity of Ni/SiO₂ system were proposed. The removal of the ligands, used in the synthesis of the colloidal Ni nanoparticles, in the post-steps of catalyst preparation is cumbersome. In fact, low temperature treatments are not able to efficiently expose the Ni surface whereas high-temperature treatments lead to particle sintering. In this systematic study several aspects of catalyst preparation through impregnation of colloidal nanoparticles are addressed.

© 2008 Elsevier B.V. All rights reserved.

1. Introduction

The main pursue in the synthesis of supported metal catalysts is to reach high metal dispersion, providing an efficient participation of the metal nanoparticles (NPs) in the catalytic processes. In several cases, however, crystalline structure and particle size of the active phase also play important roles in the catalytic performance [1–5]. As a result, the development of high active catalysts for industrial applications depends strongly on the synthetic routes and on the activation processes employed in catalyst manufacturing [6–8].

Impregnation of metal salts on supports followed by activation under a reducing atmosphere is by far the most used synthetic route to obtain supported metal catalysts for industrial processes [6]. This method quite often results in a non-uniform distribution of the active phase on the support, as reported for impregnated Ni

salts on many supports [4,9,10]. Colloidal metal NPs have been commonly invoked as promising systems to fill this lack [5,11–14]. Late transition metal NPs with controlled size and structure can be produced by modern wet chemical synthesis methods [15], opening a window of possibilities to use these NPs as building blocks for the construction of heterogeneous catalysts and to systematically relate well-characterized materials to their catalytic performance. However, just a small number of the successful examples of designed heterogeneous catalysts from colloidal NPs has been reported so far [15]. Most of these examples are catalysts containing noble metals NPs, such as Au, Pd, Ir and Pt.

Colloidal Ni NPs have shown to be potential catalysts for selective hydrogenation of α,β -unsaturated aldehydes, ketones and aromatic nitrocompounds [16–18], and for Suzuki coupling reactions [19] under quasi-homogeneous conditions. Despite the industrial importance of Ni supported catalysts, studies on the aspects involved in the utilization of colloidal Ni NPs in the construction of heterogeneous catalysts have not been reported. Here we show the results of constructing heterogeneous Ni catalysts from supports and colloidal Ni nanoparticles. The Ni supported materials were obtained by impregnating (5–10 wt%) colloidal Ni NPs on silica Aerosil or activated carbon. The obtained materials were applied to hydrogenation of cyclohexene and to steam reforming of ethanol. The thought-provoking lack of catalytic activity of Ni colloidal NPs supported on silica Aerosil was investigated in detail,

* Corresponding author. Present address: Max-Planck-Institut für Kohlenforschung, Kaiser-Wilhelm-Platz 1, 45470 Mülheim an der Ruhr, Germany. Tel.: +49 208 306 2375; fax: +49 208 309 2995.

** Corresponding author.

E-mail addresses: rinaldi@mpi-muelheim.mpg.de (R. Rinaldi), zanchet@lnls.br (D. Zanchet).

and the factors responsible for the low catalytic performance of Ni/SiO₂ system proposed.

2. Experimental

2.1. Synthesis of colloidal Ni NPs

Colloidal Ni NPs were synthesized as described elsewhere [14]. Typically, a mixture of oleic acid (OA, 0.32 mL, 1.0 mmol, 99%, Aldrich), Ni(CH₃COO)₂·4H₂O (1.00 g, 4.5 mmol, >99.0%, Fluka) and trioctylamine (TOA, 2.50 mL, 5.0 mmol, >99.0%, Fluka) in diphenyl ether (40 mL, 99%, Aldrich) was heated up to 373 K under N₂ atmosphere. At 373 K, this solution was degassed under vacuum for 90 min. In another flask, a solution of 1,2-dodecanediol (2.10 g, 11 mmol, Aldrich) in diphenyl ether (10 mL) was also prepared under inert atmosphere and degassed under vacuum at 353 K for 90 min. The Ni(II) containing solution was heated up to 453 K under N₂. At this temperature, trioctylphosphine (TOP, 0.60 mL, 1.3 mmol, >90%, Aldrich) was added at once. The reaction mixture was immediately heated up to 493 K and the 1,2-dodecanediol (hot) solution was added at once. At this point, the mixture was aged at 493 K for 20 min, resulting in a black-colored dispersion. This dispersion was cooled down to 313 K and the colloidal Ni NPs were precipitated by adding 40 mL of degassed ethanol (p.a., 99.9%, Mallinckrodt). The Ni NPs were centrifuged and washed three times with degassed ethanol, under N₂. The resulting Ni NPs were redispersed in a mixture of *n*-octane, 1-octanol and OA (95:4:1) and stored at 278 K under N₂.

2.2. Impregnation of colloidal Ni NPs

The impregnation of colloidal Ni NPs was carried out at room temperature under N₂. Typically, 0.200 g of the support, dried overnight at 473 K (Silica Aerosil 90 or active carbon Merck), were suspended in hexanes (20 mL, Mallinckrodt). This suspension was sonicated for 15 min under N₂. In sequence, 10 mL of a dispersion containing a suitable amount of Ni NPs (e.g. 10 mg for 5 wt% Ni NPs loading) were added to the support suspension. This mixture was mechanically shaken for 16 h under N₂. The solvent was removed by bubbling N₂ at 323 K and the resulting Ni/SiO₂ and Ni/C powders were stored in a dry-box under Ar.

2.3. Characterization

X-ray photoelectron spectroscopy (XPS) data was obtained with an SPECSLAB II (Phoibos-Hsa 3500 150, 9 channeltrons) SPECS spectrometer, with Al K α source ($E = 1487$ eV, $E_{\text{pass}} = 40$ eV, 0.05 eV energy step and acquisition time of 1 s per point). The samples were placed on carbon-tape under Ar. The samples were transferred under inert atmosphere to the XPS pre-chamber. The residual pressure inside the analysis chamber was smaller than 1×10^{-9} Torr. The binding energies (BE) were referenced to the C 1s or Si 2s peaks, at 284.6 or 102.6 eV, respectively, providing accuracy within ± 0.2 eV.

CO adsorption experiments and Fourier transform infrared (FT-IR) spectra were recorded using a FT-IR Thermo Nicolet 4700 Nexus spectrophotometer equipped with a diffuse reflectance reactor cell (DRIFT HTHV, CaF₂ cell, Spectra Tech). Ni/SiO₂ sample was reduced *in situ* at 423, 623 and 773 K under a 25% H₂/N₂ mixture flow for 1 h. CO adsorption was carried out at room temperature with pulses of CO (0.5 mL) at a pressure of 9 Torr. Each spectrum was collected (64 scans) after 5 min of exposure to CO.

The neat colloidal Ni NPs and supported samples were characterized by transmission electron microscopy (TEM) using a JEOL JEM 3010 microscope, operating at 300 kV (1.7 Å point resolution)

at LME-LNLS, Brazil. The supported samples were dispersed in isopropanol and deposited on amorphous carbon coated copper grids.

2.4. Catalytic reactions

Hydrogenation of cyclohexene was carried out in a stainless autoclave with magnetic stirring. All handling and transfers involved in this procedure were done under N₂. Typically, the autoclave was loaded with cyclohexene (10 mmol, 99%, Aldrich) in methanol (50 mL, p.a. Merck), 1–10 mol% of Ni, and 5 bar of H₂ at room temperature. The catalytic tests were carried out at 298–373 K and under 5–10 bar of H₂. The H₂-consumption was measured with a Huba Control pressure transducer interfaced via a Novus Field Logger converter to a computer.

Steam reforming of ethanol was carried out in a fixed bed quartz reactor operated isothermally at atmospheric pressure as described elsewhere [33]. The impregnated samples (120 mg) were pretreated *in situ* at 623 K for 3 h under H₂ flow (50 mL min⁻¹). The catalytic activity and selectivity were measured in the 470–900 K range. The reactor was continuously fed with a mixture H₂O-ethanol (6:1 mol/mol, 2 mL h⁻¹). The volatile products were analyzed in a gas chromatograph (Varian 3600 CX) equipped with a W-chromosorb column (Chrompack) and a thermal conductivity detector.

3. Results and discussion

Colloidal Ni NPs were synthesized through the reduction of Ni(CH₃COO)₂ by 1,2-dodecanediol in the presence of ligands (TOA, TOP and OA) at high temperature [14,20,21]. The Ni NPs are capped by TOA, TOP and OA, making them dispersible in non-polar solvents, such as hexanes. A given amount of this Ni NPs dispersion was added to either silica Aerosil (Ni/SiO₂) or activated carbon (Ni/C) suspended in hexanes to produce 5–10 wt% of Ni supported materials. The impregnation of Ni NPs on silica Aerosil affords a purple solid. Fig. 1 shows TEM images of the neat colloidal Ni NPs and the impregnated Ni/SiO₂ and Ni/C samples. The neat NPs of 5.3 nm (Fig. 1a) are spherical and show narrow size distribution ($\sigma = 11\%$). The Ni/SiO₂ material has a very good distribution of the particles on the support (Fig. 1b). On the other hand, the Ni NPs tend to slightly segregate in the Ni/C material (Fig. 1c).

Our first attempt to explore the catalytic properties of the supported Ni NPs was to use these materials in a model reaction, such as hydrogenation of cyclohexene. Unexpectedly, in these experiments, no catalytic activity for hydrogenation of cyclohexene at 10 bar of H₂ and 373 K was detected for both Ni/SiO₂ and Ni/C samples. In fact, this reaction proceeds quite easily using an industrial Ni-Raney catalyst under milder conditions. For instance, the hydrogenation of cyclohexene affords ca. 90% of cyclohexane after 2 h at 5 bar of H₂, 298 K and 5 mol% of Ni-Raney.

The lack of catalytic activity in the hydrogenation of cyclohexene is quite thought provoking. It is known that the catalytic performance of metal NP is strongly related to the type of capping ligands used in the colloidal synthesis [16,22]. The capping ligands are indispensable for the stabilization of the colloidal NPs as well as for the control of their size and their shape during the NP synthesis. However, these molecules can also block active sites for catalysis. Fig. 2 shows the Ni 2p core-level XP-spectra of neat colloidal Ni NPs, 5 wt% Ni/SiO₂ and 5 wt% Ni/C. The XP spectrum of the neat Ni NPs indicates that several paramagnetic Ni²⁺-species are present on the surface, as revealed by the large values of full-width at half maximum (FWHM) of the Ni 2p core-level photoemissions (ca. 3.5 eV), and by the shake-up satellite. In recent reports [14,22,23], these Ni²⁺-species were characterized as mostly formed by a disordered arrangement of few atomic layers of Ni²⁺-species, such as

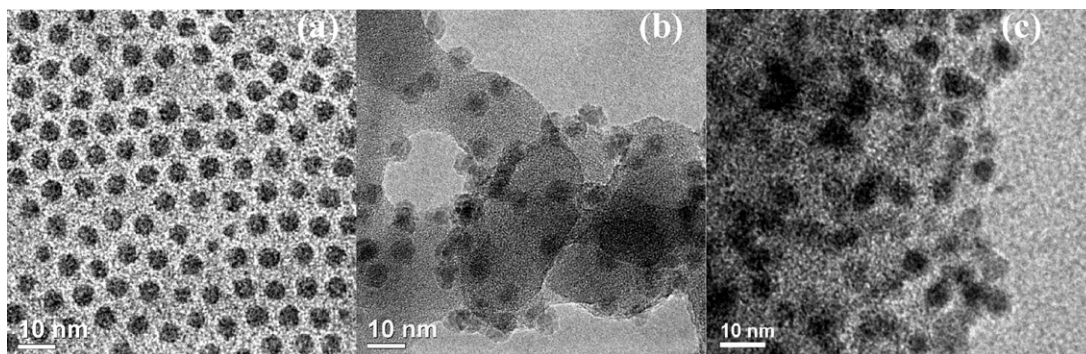


Fig. 1. TEM images of (a) colloidal Ni nanoparticles, (b) Ni/SiO₂ and (c) Ni/C.

Ni²⁺(oleate). A small contribution of Ni(0) species ($E = 852.7$ eV) is found in the neat Ni NPs sample (~12 at.%). Quantitative analysis shows that the contribution of the Ni(0) species increases from 12 to 36 at.% in the Ni/SiO₂ sample relative to the neat Ni NPs sample, suggesting that the SiO₂ surface acts as a “solid ligand”, stripping partially the capping ligands on the Ni NPs in the impregnation process. On the other hand, the Ni/C sample showed a similar XP-spectrum to the neat Ni NPs, but only negligible amount of Ni(0) species is present (Fig. 2).

To better address the phenomena involving the capping ligands on the Ni NPs and the interaction of Ni NPs with the support surfaces, O 1s and P 2p core-level XP spectra were also obtained. Fig. 3 shows the comparison of O 1s XP-spectra for the supports, C and SiO₂, and corresponding Ni NPs supported materials (Ni/C and Ni/SiO₂). While C and Ni/C samples show similar O 1s XP-spectra, in the Ni/SiO₂ sample the additional peak at 528 eV, detected in the SiO₂, is missing. This indicates that the Ni NPs are probably anchored by strong interactions involving siloxane sites on the surface of silica Aerosil [24,25].

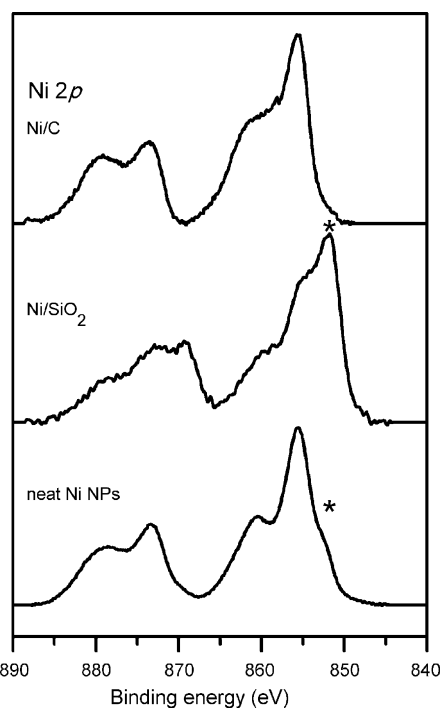


Fig. 2. Ni 2p core-level XP spectra of neat Ni NPs, and supported Ni NPs on silica and on activated carbon. The asterisks indicate Ni(0) component.

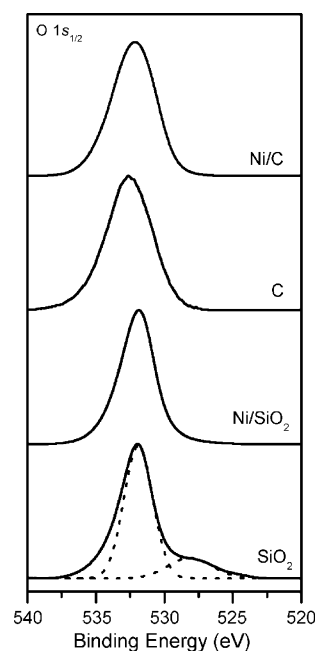


Fig. 3. O 1s core-level XP spectra of supports (C and SiO₂) and Ni/C and Ni/SiO₂ samples.

Fig. 4 shows the P 2p core-level XP-spectra of the neat Ni NPs and supported materials. The quantitative results are summarized in Table 1. Three phosphorus species were identified in the spectrum of the neat colloidal NPs. The species at 129.9 eV (P-1) is ascribed to TOP loosely bonded to the surface [26,27]. On the other hand, TOP bonded on Ni sites is assigned to the peak at 132.7 eV (P-2) [26,27]. The higher BE peak, found at 134.4 eV (P-3), is compatible to trioctylphosphine oxide (TOPO) bonded on the NPs surface [28]. Although TOPO was not used in the colloidal synthesis of Ni NPs, its formation is quite prone under presence of oxygenated molecules (e.g. 1,2-dodecanediol) at high temperatures.

Table 1

P 2p core-level XP-spectra region. The values in parenthesis are the FWHM of each component.

Material	P 2p		
	P-1	P-2	P-3
Neat Ni NPs	129.9 eV (2.4 eV), 32%	132.7 eV (2.6 eV), 42%	134.4 eV (2.6 eV), 26%
Ni/SiO ₂	–	–	–
Ni/C	–	133.2 eV (2.4 eV), 71%	134.9 (2.6 eV), 29%

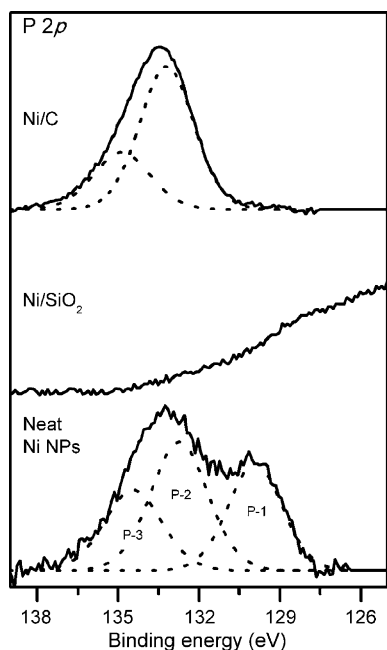


Fig. 4. P 2p core-level XP spectra of neat Ni NPs, Ni/SiO₂ and Ni/C samples.

Ni/C sample shows the peaks assigned to TOP and TOPO bonded on the Ni sites. The ratio of these species is 70:30, which is nearly close to the ratio found in the neat Ni NPs sample (62:38), when it is not taken into account the peak of loosely bonded TOP (see Table 1). The XP-spectrum of Ni/SiO₂ sample, however, shows no P 2p core-level photoelectron emission, indicating that P-ligands were stripped from the Ni NPs surface after impregnation on silica. This stripping mechanism is not completely understood at this moment, but we think that it is related to the apparent increase of Ni(0) sites observed in Fig. 3 and to the anchoring of the NPs on the Si–O–Si sites.

In an attempt to find a procedure to clean Ni NPs surface from the capping ligands utilized in the colloidal synthesis, the Ni/SiO₂ sample was studied in more details. The Ni/SiO₂ sample was treated under a reducing atmosphere (H₂:N₂ ratio of 8:38) at 423, 623 and 773 K and monitored by *in situ* DRIFTS measurements (Fig. 5).

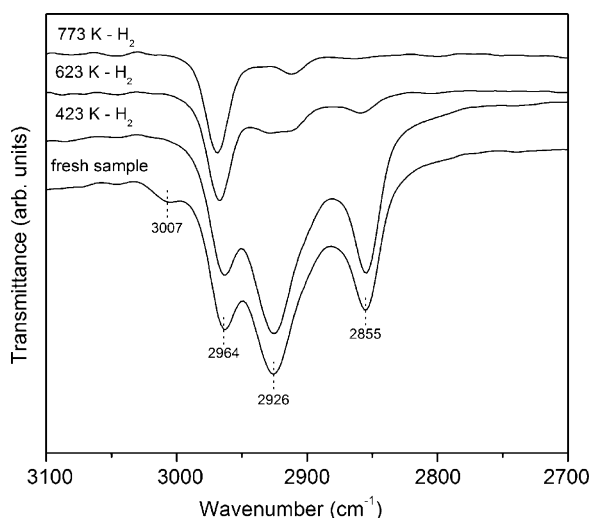


Fig. 5. DRIFT-spectra of Ni/SiO₂ fresh sample and after reduction at 423, 623 and 773 K. All spectra were taken at room temperature.

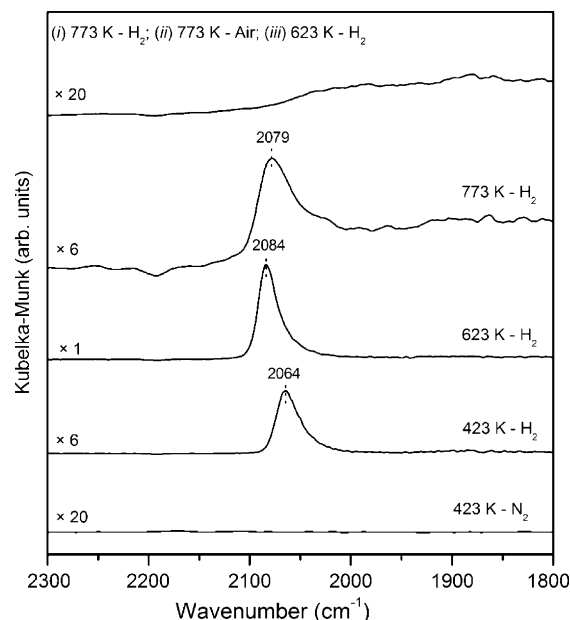


Fig. 6. DRIFT-spectra of CO adsorbed at room temperature on a Ni/SiO₂ sample treated at different temperatures (423, 623 and 773 K) and atmosphere (N₂, H₂ or air). The upper curve was obtained after treating the sample at 773 K in H₂, then in air at same temperature followed by a reduction at 623 K with H₂. Note that each curve has a different intensity scale.

The bands at 2855, 2926 and 2964 cm⁻¹ (Fig. 6) correspond to the stretching vibration bands of unsaturated C–H bonds [29] while the band at 3007 cm⁻¹ is characteristic of C=C–H stretching of OA [29]. The latter band disappears above 423 K, indicating that OA is removed, but it is also possible that the loss of the C=C–H stretching vibration is due to the hydrogenation of the C=C bond. However, significant amount of organics is still present and starts to be only removed above 623 K. Even after heating in H₂ at 773 K, considerable amount of organics still remains on the material. The complete removal of organics was only achieved under oxidant atmosphere at 773 K, when C–H stretching bands disappeared (not shown here).

An important aspect to be considered in the designing of high active Ni catalysts is the availability of Ni(0) sites to the incoming molecules. Carbon monoxide adsorption followed by FT-IR spectroscopy is a useful tool to analyze the presence of Ni(0), Ni(I), and Ni(II) sites on supported nickel catalysts [9]. Surface carbonyls of Ni(0) are stable. Typically, linear carbonyls of metallic nickel appear around 2060 cm⁻¹, whereas the bridged carbonyls are visible below 2000 cm⁻¹ [9,30,31]. The stretching frequencies of CO for surface Ni(0) carbonyls are structure sensitive, i.e., they can provide information about the crystallinity, dispersion and electrophilicity of Ni NPs on the support [9,30]. Ni(I) surface carbonyls are also stable under equilibrium CO pressures, which can be detected in the range of 2160–2110 cm⁻¹ [9,32]. Surface carbonyls of Ni(II) are not stable at room temperature. Usually, Ni(II)–CO produces bands around 2220–2180 cm⁻¹ only detectable under equilibrium pressures of CO at 85 K [9]. Fig. 6 shows the room temperature FT-IR spectra of CO adsorbed on Ni/SiO₂ sample pretreated at several temperatures and different atmospheres.

No adsorption of CO is observed in the DRIFT spectrum of the Ni/SiO₂ sample treated at 473 K under N₂. By heating at same temperature, but under H₂, a weak band of a linear bonded CO is detected at 2064 cm⁻¹. When Ni/SiO₂ sample is reduced at 623 K, the linear bonded CO band is more intense and shifted to 2084 cm⁻¹. The higher intensity of this band is in agreement with a more efficient removal of capping ligands on the Ni NPs surface

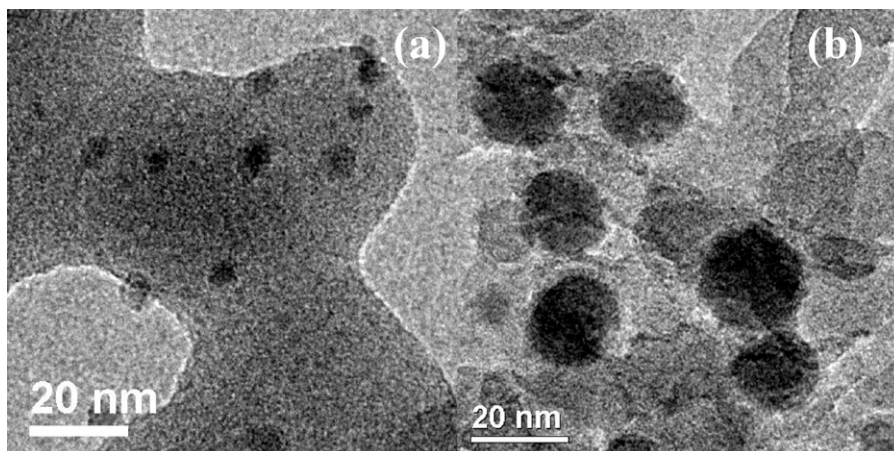


Fig. 7. TEM images of: (a) Ni/SiO₂ reduced at 623 K and (b) Ni/SiO₂ reduced at 773 K.

(Fig. 5). By reducing the sample at 773 K, a substantial decrease in the intensity of this metal-carbonyl band is seen, indicating shrinkage of the metal area due to sintering of Ni NPs (*vide infra*). In a last experiment, the Ni/SiO₂ sample was first reduced at 773 K, oxidized in air at 773 K and again reduced at 623 K. In this case, no CO band is detected in the DRIFTS spectrum, indicating that the reduction of NiO_x-species to Ni(0) requires temperatures much higher than 623 K [9].

Although high-temperature treatments can effectively reduce the amount of ligands on the NPs surface, as indicated by the FT-IR experiments, they may also increase the mobility of the NPs, favoring then the sintering. The morphological changes of the Ni NPs after impregnation and thermal treatments were analyzed by TEM (Fig. 7). As already presented in Fig. 1a, the neat colloidal Ni NPs are spherical and nearly monodisperse. The impregnation on SiO₂ Aerosil affords a good homogeneous dispersion of the Ni NPs on the SiO₂ surface (Fig. 1b). The thermal treatment of the Ni/SiO₂ sample under H₂ at 623 K (Fig. 7a) does not affect significantly the morphology of the supported Ni NPs. No evidence of NPs sintering is found at 623 K, which suggests that Ni NPs are strongly attached to the SiO₂ surface. Conversely, the thermal treatment at 773 K causes a strong sintering, as verified by the expressive growth of the NPs (~20 nm) (Fig. 7b). This is in agreement with the decreasing of the CO-band intensity in the IR spectrum for the sample treated at 773 K (Fig. 6).

A more careful analysis of the contrast of TEM images also gives complementary information. In Fig. 1a, no visible oxidation layer can be detected in the neat colloidal NPs (such as a core-shell type of contrast). On the other hand, Ni NPs supported on SiO₂ exhibits a core-shell contrast, as detected by a darker core surrounded by a lighter shell (Fig. 1b). This oxide shell is probably formed by the partial stripping of the capping ligands. The exposure to air in the sample preparation for TEM probably causes the formation of the NiO_x shell on the Ni NPs in the Ni/SiO₂ sample. On the other hand, since the neat colloidal NPs are much more protected by the capping ligands, the formation of a NiO_x shell does not happen. Likewise, Ni/C sample (Fig. 1c) shows no core-shell contrast, in agreement with the XPS results that showed no significant modification of the capping layer of ligands on the Ni NPs (Fig. 4).

The Ni/SiO₂ material was tested for steam reforming of ethanol. In this complex reaction, the activation of the reactants requires different Ni sites on each step of the process. Thereby, the analysis of the products distribution formed in this reaction can provide useful information on the availability of Ni sites on the Ni/SiO₂ sample.

The ideal catalysts for ethanol reforming has to [33,34]: (i) dehydrogenate ethanol to acetaldehyde (Eq. (1)); (ii) promote the C–C bond cleavage (Eq. (2)), resulting in CH₄ and CO; and (iii) activate water for oxidation of CH₄ and CO to CO₂ (Eqs. (3) and (4)). The promotion of hydrogenation activity is not desired for steam reforming of ethanol, since it decreases the production of H₂ due to formation of CH₄ by CO hydrogenation (methanation). Eqs. (1)–(4) represent the proposed steps of the steam reforming of ethanol process, while Eq. (5) shows the overall process stoichiometry [33,34].



The profile of the reaction products in the catalytic reaction using 10 wt% Ni/SiO₂ sample is shown in Fig. 8. The sample was previously treated under H₂ at 623 K, under similar conditions of the DRIFTS experiments. The results of ethanol reforming (Fig. 8)

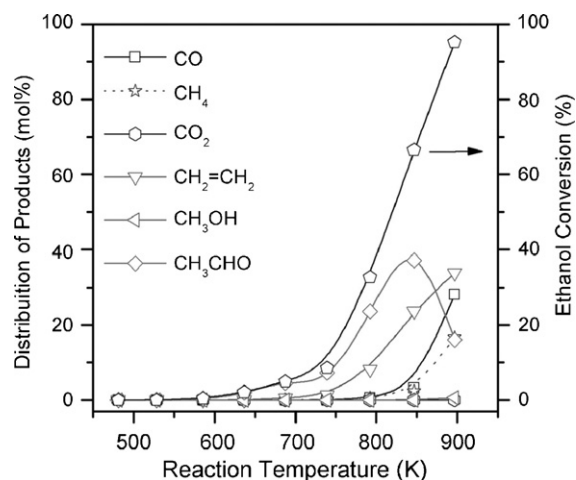


Fig. 8. Products distribution of steam reforming of ethanol. Reaction conditions: 0.120 g of catalyst (10 wt% Ni/SiO₂); reactor fed with a mixture H₂O-ethanol (6:1 mol/mol, 2 mL h⁻¹); helium was used as carrier gas.

show that the Ni sites are not highly accessible, not providing suitable catalytic sites for the cleavage of acetaldehyde to yield CO and CH₄ as indicated in Eq. (2). The Ni/SiO₂ sample is active only above 750 K. In this case, however, the molar ratio of CO:CH₄ formed is higher than 1, which indicates that the decomposition of acetaldehyde is not the only pathway of CO formation. The higher amount of CO than CH₄ is likely to be generated by the partial oxidation of coke formed on the catalyst surface [34] or oxidation of residues of NPs capping ligands. Interestingly, we observed formation of ethylene above 600 K, indicating that Ni/SiO₂ possesses acidity, probably due to formation of nickel(II) silicates [9] under the reaction conditions. It is important to remark that sintering occurs when the temperature is above 700 K, completely changing the material as the temperature is further increased (Fig. 7b).

Putting all these pieces of information together, we can get some insights on the factors responsible for the low catalytic activity of Ni NPs supported on silica. In principle, the impregnation of the Ni NPs on silica Aerosil strips mostly of the P-ligands (TOP and TOPO) as revealed by XPS (Fig. 4). However, other ligands remain strongly bonded on the Ni/SiO₂ surface as detected by DRIFTS experiments (Fig. 5). Ni NPs seem to be strongly anchored on the silica surface through siloxane groups, and no sintering of Ni NPs takes place below 623 K under a reducing atmosphere (Fig. 7).

Interestingly, while XPS revealed the presence of metallic Ni sites in the Ni/SiO₂ sample, no adsorption of CO is detected by DRIFTS and no catalytic activity is found for the untreated samples. One reasonable explanation is, despite being an outmost surface sensitive technique, XPS probes few atomic sublayers from the surface. However, the catalytic reaction and CO adsorption takes place only on the directly exposed Ni sites on the surface. Hence, this specific Ni(0) sites, detected by XPS, could not be accessible to interact with CO.

The treatment of Ni/SiO₂ under reducing atmosphere partially cleans the Ni NPs surface from the capping ligands (Fig. 5). However, it is noteworthy that only linear CO bonded is detected in the CO adsorption experiments (Fig. 6). This contrasts strongly with supported Ni catalysts obtained from impregnation of Ni salts [9,33], which also show CO bands assigned to several modes of bridged bonded CO. The interaction of the remaining capping ligands on the Ni NPs surface can change the electronic behavior of the Ni sites, restricting the coordination of CO and other small molecules.

CO adsorption experiments revealed that the Ni sites on a sample reduced at 623 K are more electrophilic than the Ni sites on a sample reduced at 423 K, since the IR-band assigned to linear bonded CO shifted from 2064 to 2084 cm⁻¹. The higher CO stretching frequency shows that the back-bonding Ni(3d) → π_{CO}^{*} is less effective, which indicates a lower electron density on Ni in Ni/SiO₂ reduced at 623 K. These changes clearly show that new interactions between the Ni NPs and the support are established during the removal of the capping ligands. The interactions involving the Ni NPs and the silica surface maintain the Ni NPs stable against sintering up to 623 K.

The construction of catalyst from supports and colloidal nanoparticles is a much more complex process than the conventional impregnation of metal salts followed by reducing steps. The removal of the capping ligands, which are essential for tailoring the properties of nanoparticles in the colloidal synthesis, is the central challenge that remains to be circumvented in the case of late 3d metal NPs. The main problem to be solved is to remove the capping ligands without oxidizing the NPs surface. This is very required, since the oxides of late 3d metals usually are reduced at high temperatures (e.g. NiO_x-species reduces to Ni(0) above 700 K [9]). At these temperatures, the sintering processes are rather prone to occur, destroying all the properties tailored by the colloidal synthesis of NPs.

4. Conclusions

We have explored the potential use of colloidal Ni NPs supported in silica and activated carbon as catalyst for hydrogenation of cyclohexene and for steam reforming of ethanol. Despite the homogenous size of the colloidal Ni NPs, this synthetic route was not successful to provide active Ni catalysts. The impregnation of Ni NPs on silica resulted in high metal dispersion, which would provide an efficient participation of the supported NPs in the catalytic processes. However, the application in the hydrogenation of cyclohexene and in the steam reforming of ethanol revealed a lack of catalytic activity. The detailed surface analysis of the Ni/SiO₂ sample showed that the capping-ligands are not easily and fully removed from the Ni surface in the posterior steps of catalyst preparation, inhibiting the surface to activation of reactants. This has been shown particularly important for the case of Ni catalysts as studied here, because other catalysts produced by impregnation of Ni salts resulted in active materials for steam reforming of ethanol [33]. The interaction between silica Aerosil surface and Ni NPs is strong enough to partially displace the capping ligands, efficiently grafting the Ni NPs on the silica surface, which avoids the Ni NPs sintering even at 623 K. However, this interaction could not provide a suitable Ni surface for catalysis. Further studies in a broader set of colloidal systems are desirable to draw a better picture of the potential use of this methodology in the rational design of catalysts.

Acknowledgments

LME-LNLS is acknowledged for the use of TEM. R.R. is grateful to CNPq for the post-doc fellowship at the LNLS facilities and to Mr. Fabio Zambello for his assistance in part of this work.

References

- [1] Y.H. Cui, H.Y. Xu, Q.J. Ge, Y.Z. Wang, S.F. Hou, W.Z. Li, J. Mol. Catal. A: Chem. 249 (2006) 53.
- [2] H. Wilmer, M. Kurtz, K.V. Klementiev, O.P. Tkachenko, W. Grunert, O. Hinrichsen, A. Birkner, S. Rabe, K. Merz, M. Driess, C. Woll, M. Muhler, Phys. Chem. Chem. Phys. 5 (2003) 4736.
- [3] A.J. Nagy, G. Mestl, R. Schlögl, J. Catal. 188 (1999) 58.
- [4] G. Pina, C. Louis, M.A. Keane, Phys. Chem. Chem. Phys. 5 (2003) 1924.
- [5] R. Schlögl, S.B.H. Abd, Angew. Chem. Int. Ed. 43 (2004) 1628.
- [6] J.A. Schwarz, C. Contescu, A. Contescu, Chem. Rev. 95 (1995) 477.
- [7] J.R.A. Sietsma, J.D. Meeldijk, M. Versluijs-Helder, A. Broersma, A.J. van Dillen, P.E. de Jongh, K.P. de Jong, Chem. Mater. 20 (2008) 2921.
- [8] J.R.A. Sietsma, J.D. Meeldijk, J.P. den Breejen, M. Versluijs-Helder, A.J. van Dillen, P.E. de Jongh, K.P. de Jong, Angew. Chem. Int. Ed. 46 (2007) 4547.
- [9] K. Hadjiivanov, M. Mihaylov, D. Klissurski, P. Stefanov, N. Abadjieva, E. Vassileva, L. Mintchev, J. Catal. 185 (1999) 314.
- [10] A. Infantes-Molina, J. Merida-Robles, P. Braos-Garcia, E. Rodriguez-Castellon, E. Finocchio, G. Busca, P. Maireles-Torres, A. Jimenez-Lopez, J. Catal. 225 (2004) 479.
- [11] G.A. Somorjai, F. Tao, J.Y. Park, Top. Catal. 47 (2008) 1.
- [12] R. Narayanan, M.A. El-Sayed, Top. Catal. 47 (2008) 15.
- [13] J. Park, E. Kang, S.U. Son, H.M. Park, M.K. Lee, J. Kim, K.W. Kim, H.J. Noh, J.H. Park, C.J. Bae, J.G. Park, T. Hyeon, Adv. Mater. 17 (2005) 429.
- [14] H. Winnischofer, T.C. Rocha, W.C. Nunes, L.M. Socolovsky, M. Knobel, D. Zanchet, ACS Nano. 2 (2008) 1313.
- [15] Y. Zhu, C.N. Lee, R.A. Kemp, N.S. Hosmane, J.A. Maguire, Chem. Asian J. 3 (2008) 650.
- [16] B.J. Liaw, S.J. Chiang, C.H. Tsai, Y.Z. Chen, Appl. Catal. A: Gen. 284 (2005) 239.
- [17] S.J. Chiang, B.J. Liaw, Y.Z. Chen, Appl. Catal. A: Gen. 319 (2007) 144.
- [18] R. Xu, T. Xie, Y. Zhao, Y. Li, Nanotechnology 18 (2007) 055602.
- [19] J. Park, E. Kang, S.U. Son, H.M. Park, M.K. Lee, J. Kim, K.W. Kim, H.-J. Noh, J.-H. Park, C.J. Bae, J.-G. Park, T. Hyeon, Adv. Mater. 17 (2005) 429.
- [20] J. Yang, T.C. Deivaraj, H.P. Too, J.Y. Lee, Langmuir 20 (2004) 4241.
- [21] D. Li, S. Komarneni, J. Am. Soc. 89 (2006) 1510.
- [22] C.A. Stowell, B.A. Korgel, Nano Lett. 5 (2005) 1203.
- [23] G.G. Couto, J.J. Klein, W.H. Schreiner, D.H. Mosca, A.J.A. Oliveira, A.J.G. Zarbin, J. Colloid Interf. Sci. 311 (2007) 461.
- [24] A. Opitzka, S.I.-U. Ahmedb, J.A. Schaefera, M. Scherge, Wear 254 (2003) 924.
- [25] B. Hornetz, H.-J. Michel, J. Halbritter, J. Mater. Res. 9 (1994) 3088.
- [26] M.C. Oliveira, A.M.B. Rego, J. Alloys Compd. 425 (2006) 64.
- [27] J. Pinkas, Z. Bastl, M. Slouf, J. Podlaha, P. Stepanicka, New J. Chem. 25 (2001) 1215.

- [28] W.E. Morgan, W.J. Stec, J.R. van Wazer, *Inorg. Chem.* 12 (1973) 953.
- [29] N. Wu, L. Fu, M. Su, M. Aslam, K.C. Wong, V.P. Dravid, *Nano Lett.* 4 (2004) 383.
- [30] J.T. Yates, C.W. Garland, *J. Phys. Chem.* 65 (1961) 617.
- [31] C.W. Garland, R.C. Lord, P.F. Troiano, *J. Phys. Chem.* 69 (1965) 1195.
- [32] L. Bonneviot, F.X. Cai, M. Che, M. Kermarec, O. Legendre, C. Lepetit, D. Olivier, *J. Phys. Chem.* 91 (1987) 5912.
- [33] J.W.C. Liberatori, R.U. Ribeiro, D. Zanchet, F.B. Noronha, J.M.C. Bueno, *Appl. Catal. A: Gen.* 327 (2007) 197.
- [34] N.V. Parizotto, K.O. Rocha, S. Damyanova, F.B. Passos, D. Zanchet, C.M.P. Marques, J.M.C. Bueno, *Appl. Catal. A: Gen.* 330 (2007) 12.